

# Interface-Controlled, High-Mobility Organic Transistors\*\*

By Oana D. Jurchescu, Mihaita Popinciuc, Bart J. van Wees, and Thomas T. M. Palstra\*

Electronic devices based on organic semiconductors have gained considerable industrial and academic interest in recent years.<sup>[1–17]</sup> Organic materials present new semiconductors for flexible, low-cost, and light-weight electronic devices. Pentacene has become a prominent choice for both industrial applications as well as fundamental studies. The device functionality remains limited by the relatively low electron mobility, which, for thin-film devices, is partially caused by a large grain-boundary resistance.<sup>[18]</sup> Rapid technological progress has been made in the fabrication of field-effect transistors (FETs) at the organic semiconductor surface,<sup>[19–24]</sup> however, the electron mobility of such FET devices is typically much smaller than that which can be obtained in bulk materials.<sup>[25–27]</sup> We demonstrate that this is related to the surface properties of the crystal. We use a new method to deactivate the impurity states at the interface in single-crystal devices by incorporating them into the dielectric gate barrier. In this manner, high-mobility devices can be reproducibly constructed, in which bulk mobility, evaluated from space-charge limited current (SCLC) measurements, is reached.

Recent progress in organic single-crystal FET devices has shown that the surface layer of the semiconductor, which forms the conduction channel between the source and the drain electrode, contains a broad distribution of interface states.<sup>[2]</sup> To minimize the trap density, organic dielectrics (e.g., parylene) have been used as gate dielectric.<sup>[1,19,20,25]</sup> Previous attempts, which made use of more robust dielectrics such as SiO<sub>2</sub> and Al<sub>2</sub>O<sub>3</sub>, involved too many chemical reactions and led to structural disorder. Nevertheless, even organic dielectrics often yield limited mobilities, which is partially attributed to damage below the metal electrodes.<sup>[5]</sup> However, little detailed knowledge is available on the nature of the defect states and traps. The mobility of such high-purity organic field-effect transistors (OFETs) is usually much lower than the value

determined from SCLC measurements. This can be attributed to the fact that in FET devices the surface conduction is measured, whereas the bulk mobility is probed in SCLC measurements. The bulk mobility can be increased by reducing the number of traps through controlled processing. We have chosen to investigate pentacene. This material is used for rollable displays in prototypes of commercial devices<sup>[3]</sup> and exhibits the highest reported electronic mobility: 35 cm<sup>2</sup> V<sup>-1</sup> s<sup>-1</sup> at room temperature<sup>[27]</sup> in bulk single crystals. However, a charge-carrier mobility ( $\mu$ ) value of 0.3 cm<sup>2</sup> V<sup>-1</sup> s<sup>-1</sup> was measured for FET devices built on pentacene crystals using a parylene gate dielectric.<sup>[25]</sup> This value was improved to 2.2 cm<sup>2</sup> V<sup>-1</sup> s<sup>-1</sup> for purified pentacene.<sup>[7]</sup> A mobility of 1.4 cm<sup>2</sup> V<sup>-1</sup> s<sup>-1</sup> was measured for pentacene single crystals using a SiO<sub>2</sub> gate dielectric that was treated with self-assembled monolayers.<sup>[26]</sup> The different mobilities of the bulk compared to FET devices built on pentacene single crystals indicate the necessity of a structurally and chemically clean interface. The morphology, spatial ordering, and roughness at the interface are as important as the purity of the active area of the devices.<sup>[13–15]</sup>

Our OFETs, fabricated using the method described in the Experimental, have typical charge-carrier mobility values in the range of 15–40 cm<sup>2</sup> V<sup>-1</sup> s<sup>-1</sup> at room temperature, similar to the values measured in bulk, ultrapure single crystals.<sup>[27]</sup> The on/off ratios are as high as  $I_{\text{on}}/I_{\text{off}} = 10^6$ . The large mobility values and high on/off ratios result from a reduction in the number of scattering sites at the interface between the semiconductor and insulator. The method developed in this Communication leads to remarkably good reproducibility of the devices.

We have previously established that 6,13-pentacenequinone (PQ) constitutes the largest impurity fraction in pentacene single crystals.<sup>[27]</sup> Pentacene is usually synthesized from PQ, and thus small fractions of the quinone can be recovered in the final reaction product. The purity of the material can be improved by repeated vapor-transport crystallization.<sup>[20]</sup> In typical crystal, PQ may be present at a concentration of 0.11 %, and even after repeated distillation we observed a fraction of 0.028 %.<sup>[27]</sup> Thus far it has been commonly assumed that the impurity is evenly distributed throughout the lattice. We demonstrate that this is not the case, and that PQ is in fact located preferentially at the surface. This is reasonable and can be expected from the dynamics of the crystal-growth process. Also, the quinone is easily formed by oxidation of the relatively reactive conjugated pentacene molecule. At the interface, PQ molecules form scattering centers that reduce the mobility, or even prevent transistor action alto-

[\*] Prof. T. T. M. Palstra, Dr. O. D. Jurchescu  
Solid State Chemistry Laboratory, Materials Science Center  
University of Groningen  
Nijenborgh 4, 9747 AG Groningen (The Netherlands)  
E-mail: t.t.m.palstra@rug.nl

M. Popinciuc, Prof. B. J. van Wees  
Physics of Nanodevices, Materials Science Center  
University of Groningen  
Nijenborgh 4, 9747 AG Groningen (The Netherlands)

[\*\*] We thank P. Blom, M. Mulder, and J. Harkema for the use of their evaporation equipment. This work was supported by the MSCplus (Materials Science Center) and FOM (Stichting voor Fundamenteel Onderzoek der Materie).

gether. However, PQ can be incorporated into the gate dielectric by growing additional quinone layers epitaxially on the surface. Thus, the PQ can form a pinhole-free gate barrier and considerably minimize the trap states.

Pentacene is a layered material that is characterized by a herringbone pattern within the layers; adjacent layers are bonded by van der Waals forces. Pentacene has several polymorphs, each with a particular  $d(001)$ -spacing along the  $c^*$ -axis. This length varies from 14.1 to 15.5 Å, but is unique for pentacene single crystals:  $d_P(001) = 14.1$  Å.<sup>[28]</sup> This polymorph is already adopted in the first monolayers. The  $d(001)$  spacing is significantly different in 6,13-pentacenequinone:  $d_{PQ}(001) = 17.79$  Å.<sup>[29]</sup> This allows us to distinguish the two types of molecules present at the surface by atomic force microscopy (AFM) experiments.

To characterize the surface morphology of pentacene single crystals, we investigated several crystals by using the AFM technique. We measured on different areas of the crystals. We observed terraces at the surface (see Fig. 1) that exhibited step heights with, predominantly, two values:  $(14.1 \pm 0.5)$  Å and  $(17.79 \pm 0.75)$  Å. The former value corresponds to the  $d$ -spacing of single-crystal pentacene, and the latter to that of PQ. As a reference, we studied the surfaces of the same crystals after cleavage (i.e., the bulk material). There, we observed only terraces with  $(14.1 \pm 0.5)$  Å steps, characteristic of pentacene.

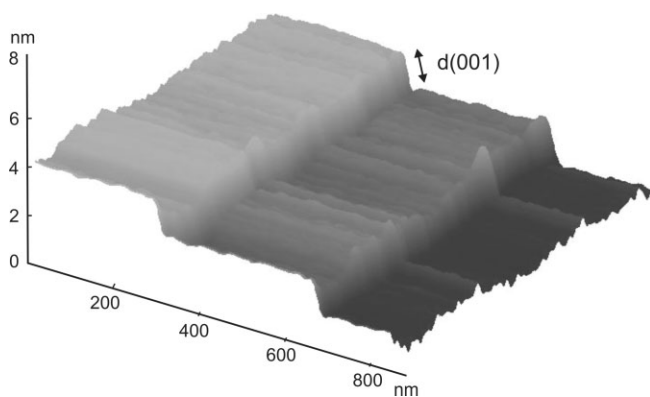


**Figure 1.** AFM picture at the surface of a pentacene single crystal, showing characteristic steps. The step height coincides with the interlayer separation distance  $d(001)$ .

We conclude that the impurities (PQ molecules) agglomerate in patches that are distributed over the surface of the pentacene crystals (see Fig. 2a). Although we have no detailed quantitative analysis over the entire crystal, we observe that the 14.1 Å step occurs approximately five times more often than the 17.79 Å step (see Experimental section). The results

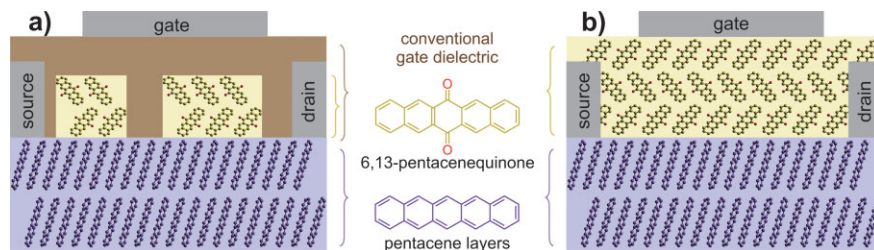


**Figure 2.** Schematic cross section of a field-effect transistor fabricated on a pentacene single crystal. The bond-line chemical formulae for 6,13-pentacenequinone (PQ) and pentacene (P) are drawn. a) Conventional gate dielectric deposited onto the surface of the pentacene crystal. Here, pentacenequinone molecules present at the interface form scattering sites and decrease the mobility. b) P–PQ OFET. Highly ordered pentacenequinone films act as gate insulators and reduce the number of scattering sites at the interface.

differ slightly between crystals, depending on the measured surface area. Similar effects were reported for acenes with a lower number of benzene rings. Quantitative analysis on tetracene single crystals, via gas chromatography (GC), allowed the detection of the tetracenequinone surface concentration, which was one order of magnitude larger than in the bulk.<sup>[30]</sup> Because the quinone is preferentially located at the surface in both pentacene and tetracene, more scattering sites are formed in the FET geometry than we determined for the bulk.<sup>[27]</sup> This is critical for the performance of the FETs, because the traps are located at the interface with the gate insulator where the active channel forms.

In the case of OFETs built on the surface of pentacene single crystals by using conventional methods (Fig. 2a),<sup>[7,25,26]</sup> the charge transport is dominated by disorder, and thus the mobility is lower than the bulk value. We assign this reduction to the presence of pentacenequinone molecules at the surface. The interactions between the  $\pi$ -systems of the “host” and the “impurity” molecules introduce additional scattering sites to the inevitable traps formed during the deposition of the gate insulator. The electric field applied at the gate electrode first has to fill these trap states. Only a higher gate bias can populate the density of states (DOS) of pentacene, and modulate the drain current for proper FET operation. Moreover, random dipoles and quadrupoles<sup>[31]</sup> are locally introduced at the interface as a result of the presence of the impurity molecules. This leads to energetic disorder, and an increase in carrier localization by electronic polarization. It has been shown by Lang et al.<sup>[2]</sup> that even high-quality pentacene single crystals have a relatively broad distribution of states (ca. 1 eV) above the edge of the valence band. The different intermolecular interactions between pentacene, pentacenequinone, and the gate insulator material modulate the energy levels of the states. This results in a broadening of the DOS, and the formation of an increased number of tail states.

We replaced the conventional gate dielectrics (e.g., SiO<sub>2</sub>, parylene, polymers) with ordered pentacenequinone films (P–PQ OFET, Fig. 2b). This method presents the unique advantage of being able to transform the scattering sites present at the surface of the single crystals into a uniform, high-quality

ity semiconductor/gate interface. In this device, the electric field applied at the gate is able to inject directly into the DOS of pentacene. This is reflected by a smaller value of the threshold voltage ( $V_T = \pm 2$  V) for devices built according to the geometry in Figure 2b, compared with devices fabricated by conventional methods ( $V_T = 5$  V, reported by Ramirez and co-workers,<sup>[25]</sup> and  $V_T = -10$  V, reported by Batlogg and co-workers<sup>[26]</sup>).

The transistors built by using the method presented here, on the surface of ultrapure pentacene single crystals, exhibit p-type conduction. We did not observe ambipolar transport for this configuration. The sharp increase in drain current ( $I_D$ ) in the transfer characteristics, presented in Figure 3a, is a typical feature of a high-performance FET device. We calculated the field-effect mobility  $\mu$  from the transconductance  $g_m = \partial I_D / \partial V_G$ , at low drain voltages  $V_D$  (Fig. 3a) using Equation 1:

$$\mu = \frac{L}{W} \frac{1}{C_i} \frac{1}{V_D} \left( \frac{\partial I_D}{\partial V_G} \right) \Big|_{V_D \rightarrow 0} \quad (1)$$

where  $L$  is the channel length,  $W$  is the gate width, and  $C_i$  is the capacitance per unit area of the gate insulator. We observe typical mobilities in the range of  $15\text{--}40 \text{ cm}^2 \text{ V}^{-1} \text{ s}^{-1}$  for the transistors fabricated using the PQ gate dielectric. The variations in mobility are caused by differences in crystal quality and contact resistance. The on/off ratio is of the order of  $10^6$ . We measured 20 devices built on eight different crystals and observed consistent behavior. The normalized subthreshold slope ( $S_i = S C_i$ , where  $S = \partial(\log I_D) / \partial V_G$ ) has a value of  $33.7 \text{ V nF decade}^{-1} \text{ cm}^{-2}$ . This value is higher, by a factor of 6–8, than the value obtained for the best rubrene transistors.<sup>[19]</sup> The quality of the manually deposited contacts is not very good, and this is reflected in the  $I$ - $V$  characteristics of even the best devices. As a result, the contacts are not equivalent and the device shows an asymmetry between  $V_D = +1$  V and  $V_D = -1$  V.

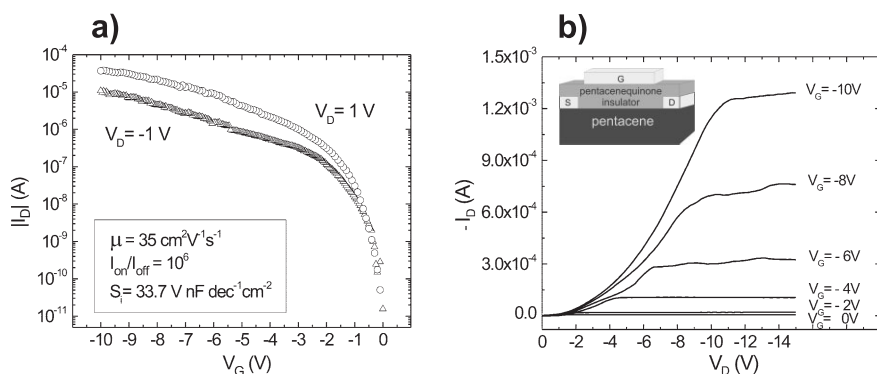


**Figure 3.** OFET fabricated on a high-purity pentacene single crystal with a 250 nm thick pentacenequinone film gate dielectric. The geometry of the device is  $L \times W = 250 \mu\text{m} \times 4 \text{ mm}$ . a) Variation of the drain current ( $I_D$ ) with respect to the applied gate voltage ( $V_G$ ), relative to the source contact for  $V_D = 1$  V and  $V_D = -1$  V. The properties of the transistor are included in the inset. b) Drain current ( $I_D$ ) versus drain voltage ( $V_D$ ) for different negative gate voltages. The inset shows the transistor geometry.

Typical output characteristics of the P-PQ transistors are plotted in Figure 3b. The current in the channel increases as the negative gate bias ( $V_G$ ) is increased and saturates at  $V_D = V_G - V_T$ . We attribute the nonlinearities in the low  $V_D$  regime to the contact-injection issues. This is consistent with previous studies that assigned superquadratic-like behavior at low drain voltages to a Schottky barrier between the Fermi level of the metal contact and the highest occupied molecular orbital (HOMO) of the p-type organic semiconductor (lowest occupied molecular orbital (LUMO) in the case of electron conduction),<sup>[32]</sup> to (diffusion-limited) thermionic emission and recombination at the metal/organic interface,<sup>[33]</sup> or to the presence of a depletion area in the vicinity of the “top contacts”, with a high density of localized states that induce a parasitic resistance in the FET circuit.<sup>[5,34,35]</sup> Because of similar experimental  $I$ - $V$  characteristics between OFETs and metal oxide semiconductor field-effect transistors (MOSFETs), we have used this theory in modeling the OFET behavior. The field-effect mobility, estimated from Figure 3b, reproduces the values obtained from the transconductance at low drain voltages. At higher drain voltages, in the linear regime as well as in the saturation regime, the value estimated from this graph represents an overestimation of the real value as a result of complementary contributions. Moreover, it increases with the gate voltage. This feature has also been reported by Goldman et al.<sup>[26]</sup> and Podzorov et al.<sup>[1]</sup> The overestimation of the mobility value can be caused by the contribution of the leakage current. Pentacenequinone is not as robust as an inorganic insulator. For an enhanced performance of the pentacene single-crystal FETs, the insulator pentacenequinone may be used as an interface layer between the organic crystal and the actual gate insulator. This presents distinct advantages: the inactivation of the scattering sites at the surface of the crystal, the presence of a dielectric with low dielectric constant where the active channel forms,<sup>[14]</sup> and the possibility of deposition of the inorganic robust dielectric by protection against the damage at the surface.

The method that we introduced for the fabrication of high-mobility pentacene transistors may be applied for the fabrication of FETs of similar materials. Surface oxidation is widely encountered in conjugated organic materials. Pentacene is highly susceptible to oxidation at the most reactive positions, leading to 6,13-pentacenequinone. The larger acenes are even less stable. The attachment of substituents on the acene backbone (e.g., phenyl in the case of rubrene) makes these positions less reactive and protects the molecule from unwanted oxidation. In this case the interaction of oxygen with the crystal is significantly different; the oxidation is reversible yielding endoperoxide instead of quinones.<sup>[36]</sup>

In conclusion, we have been able to incorporate the interface-scattering centers of PQ into the gate dielectric of organic field-effect transistors built on pentacene single crystals. In this manner, we have obtained a semiconductor/dielectric interface of extremely high quality. The field-effect transistor mobility,  $\mu = 15\text{--}40 \text{ cm}^2 \text{ V}^{-1} \text{ s}^{-1}$ , can reproduce the value obtained in ultrapure single-crystal bulk devices. This demonstrates that we were able to measure the intrinsic properties of the single crystal by careful control of the interface properties, which implies minimizing the trap density in the active channel.

### Experimental

**Single-Crystal Growth:** Pentacene single crystals with a high degree of purity were grown by using physical vapor transport [6]. The starting material was obtained from Sigma–Aldrich and was purified by using vacuum sublimation under a temperature gradient. Details concerning this step have been described elsewhere [27]. The crystal growth was performed in a horizontal glass tube under a flow of argon and a temperature gradient. The tube was cleaned and heated at 350 °C for 15 h to remove the solvents. The powder, from which the volatile impurities were removed, was placed in the hottest part of the tube, in an alumina boat. Additional purification was applied to the transporting gas by insertion of an aluminium oxide/hydrogen-activated BTS drying column (Merck, Germany). The sublimation temperature, 280 °C, was kept as low as possible in order to obtain a low crystallization rate that ensured a minimum formation of defects and avoided side reactions [7]. The setup was placed in the dark to protect against oxidation. This growth method yields platelets of pentacene single crystals with in-plane dimensions of 1–4 cm and thicknesses of 10–50  $\mu\text{m}$ .

**AFM Measurements:** The AFM measurements were performed in tapping mode using a NanoScope IV multimode scanning probe microscope from Digital Instruments. The as-grown crystals were measured first. Steps characteristic of pentacene and pentacenequinone were detected. The occurrence of the 14.1 Å and 17.79 Å steps at the surface of the pentacene single crystals, corresponding to pentacene and pentacenequinone, respectively, is shown in Figure 4a. The crystals were then cleaved, and the new surface was mapped. Only the step corresponding to pentacene was detected (Fig. 4b).

**Device Preparation:** We paid special attention to the fabrication of the FETs on the organic crystal surface, to avoid damaging the surface of the semiconductor. Silver–epoxy source and drain contacts were painted onto the crystal. A film of PQ was deposited on top. The deposition of the insulator was carried out in high vacuum ( $10^{-7}$  mbar; 1 mbar = 100 Pa) in a clean environment, and the growth was carefully controlled. The sublimation rate was low ( $5 \text{ Å min}^{-1}$ ), to ensure homogeneity of the film. The thickness was determined very precisely during the growth by using a quartz crystal balance. Calibration of the thickness measurements was preliminary performed with a Dektak profilometer (Dektak 6M Stylus Profiler, Veeco Instruments). The silver–epoxy gate electrode was then painted on top of the device.

**Device Characterization:** FET measurements were performed in the dark and under a vacuum of  $10^{-6}$  mbar [8] in a home-built probe station. The two-terminal configuration was used. The characterization was done by using a Hewlett–Packard 4155B semiconductor parameters analyzer. We investigated 20 FETs built on eight pentacene single crystals obtained from different batches. The electrical properties of the devices were similar. Small shifts in the value of the threshold voltage were recorded for different devices.

We performed  $I$ – $V$  measurements on pentacenequinone single crystals in order to estimate the electrical breakdown field of the gate dielectric. We obtained a value of ca.  $3 \text{ MV cm}^{-1}$  for the PQ single crystal insulator. Pinhole-free insulation was obtained for film thicknesses

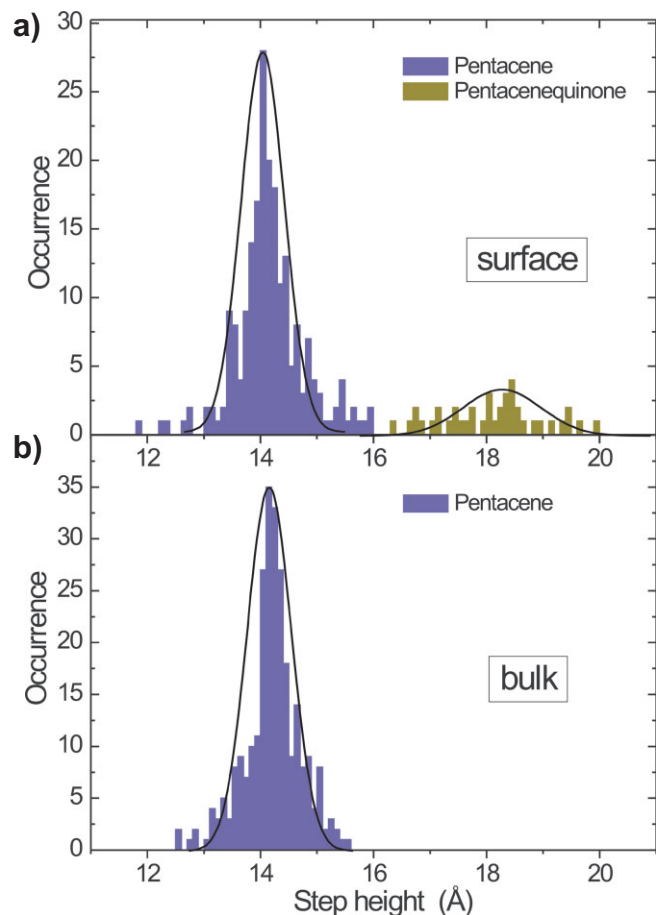


**Figure 4.** a) Occurrence of the 14.1 and 17.79 Å steps at the surface of the pentacene single crystals. The Gaussians peaking at 14.1 Å and 17.79 Å are a guide to the eye. b) Step-distribution characteristics for the bulk (obtained after cleaving the crystals), where the 14.1 Å step is observed.

greater than 200 nm. For the determination of the dielectric constant, we performed capacitance measurements on single crystals of the PQ gate dielectric material:  $\epsilon_r(\text{PQ}) = 3.5$ . An Andeen–Hagerling 2500A ultra precision capacitance bridge was used for the dielectric measurements performed on pentacenequinone and a Keithley 237 source measure unit was used to determine the insulator breakdown voltage.

Received: April 28, 2006

Revised: September 7, 2006

Published online: February 1, 2007

- [1] V. Podzorov, S. E. Sysoev, E. Loginova, V. M. Pudalov, M. E. Gershenson, *Appl. Phys. Lett.* **2003**, *83*, 3504.
- [2] D. V. Lang, X. Chi, T. Siegrist, A. M. Sergent, A. P. Ramirez, *Phys. Rev. Lett.* **2004**, *93*, 086 802.
- [3] G. H. Gelinck, H. E. A. Huitema, E. van Veenendaal, E. Cantatore, L. Schrijnemakers, J. B. P. H. van der Putten, T. C. T. Geuns, M. Beenhakkers, J. B. Giesbers, B. H. Huisman, E. J. Meijer, E. M. Benito, F. J. Touwslager, A. W. Marsman, B. J. E. van Rens, D. M. de Leeuw, *Nat. Mater.* **2004**, *3*, 106.
- [4] A. Troisi, G. Orlandi, *Phys. Rev. Lett.* **2006**, *96*, 086 601.
- [5] R. W. I. de Boer, A. F. Morpurgo, *Phys. Rev. B: Condens. Matter Mater. Phys.* **2005**, *72*, 073 207.

- [6] A. Laudise, C. Kloc, P. Simpkins, T. Siegrist, *J. Cryst. Growth* **1998**, 187, 449.
- [7] L. B. Roberson, J. Kowalik, L. M. Tolbert, C. Kloc, R. Zeis, X. L. Chi, R. Fleming, C. Wilkins, *J. Am. Chem. Soc.* **2005**, 127, 3069.
- [8] O. D. Jurchescu, J. Baas, T. T. M. Palstra, *Appl. Phys. Lett.* **2005**, 87, 052 102.
- [9] F.-J. Meyer zu Heringdorf, M. C. Reuter, R. M. Tromp, *Nature* **2001**, 412, 517.
- [10] R. Ruiz, A. Papadimitratos, A. C. Mayer, G. G. Malliaras, *Adv. Mater.* **2005**, 17, 1795.
- [11] D. A. da Silva Filho, E. G. Kim, J.-L. Brédas, *Adv. Mater.* **2005**, 17, 1072.
- [12] J. E. Northrup, M. L. Chabynec, *Phys. Rev. B: Condens. Matter Mater. Phys.* **2003**, 68, 041 202.
- [13] R. W. de Boer, N. N. Iosad, A. F. Stassen, T. M. Klapwijk, A. F. Morpurgo, *Appl. Phys. Lett.* **2005**, 86, 032 103.
- [14] A. F. Stassen, R. W. de Boer, N. N. Iosad, A. F. Morpurgo, *Appl. Phys. Lett.* **2004**, 85, 3899.
- [15] J. Veres, S. D. Ogier, S. W. Leeming, D. C. Cupertino, S. M. Khaffaf, *Adv. Funct. Mater.* **2003**, 13, 199.
- [16] B. Crone, A. Dodabalapur, Y.-Y. Lin, R. W. Filas, Z. Bao, A. LaDuca, R. Sarpeshkar, H. E. Katz, W. Li, *Nature* **2000**, 403, 521.
- [17] L.-L. Chua, J. Zaumseil, J.-F. Chang, E. C.-W. Ou, P. K.-H. Ho, H. Sirringhaus, R. H. Friend, *Nature* **2005**, 434, 194.
- [18] S. F. Nelson, Y. Y. Lin, D. J. Gundlach, T. N. Jackson, *Appl. Phys. Lett.* **1998**, 72, 1854.
- [19] V. C. Sundar, J. Zaumseil, V. Podzorov, E. Menard, R. L. Willett, T. Someya, M. E. Gershenson, J. A. Rogers, *Science* **2004**, 303, 1644.
- [20] R. W. de Boer, M. E. Gershenson, A. F. Morpurgo, V. Podzorov, *Phys. Status Solidi A* **2004**, 201, 1302.
- [21] M. Halik, H. Klauk, U. Zschieschang, G. Schmid, C. Dehm, M. Schutz, S. Maisch, F. Effenberger, M. Brunnbauer, F. Stellacci, *Nature* **2004**, 431, 963.
- [22] S. Kobayashi, T. Nishikawa, T. Takenobu, S. Mori, T. Shimoda, T. Mitani, H. Shimotani, N. Yoshimoto, S. Ogawa, Y. Iwasa, *Nat. Mater.* **2004**, 3, 317.
- [23] G. Horowitz, *Adv. Mater.* **1998**, 10, 365.
- [24] C. D. Dimitrakopoulos, P. R. L. Malenfant, *Adv. Mater.* **2002**, 14, 99.
- [25] V. Y. Butko, X. Chi, D. V. Lang, A. P. Ramirez, *Appl. Phys. Lett.* **2003**, 83, 4773.
- [26] C. Goldmann, S. Haas, C. Krellner, K. P. Pernstich, D. J. Gundlach, B. Batlogg, *J. Appl. Phys.* **2004**, 96, 2080.
- [27] O. D. Jurchescu, J. Baas, T. T. M. Palstra, *Appl. Phys. Lett.* **2004**, 84, 3061.
- [28] C. C. Matheus, A. B. Dros, J. Baas, A. Meetsma, J. L. de Boer, T. T. M. Palstra, *Acta Crystallogr., Sect. C: Cryst. Struct. Commun.* **2001**, 57, 939.
- [29] A. V. Dzyabchenko, V. E. Zavodnik, V. K. Belsky, *Acta Crystallogr., Sect. B: Struct. Sci.* **1979**, 35, 2250.
- [30] J. Pflaum, J. Niemax, A. K. Tripathi, *Chem. Phys.* **2006**, 325, 152.
- [31] C. A. Hunter, J. M. Sanders, *J. Am. Chem. Soc.* **1990**, 112, 5525.
- [32] V. I. Arkhipov, E. V. Emelianova, Y. H. Tak, H. Bässler, *J. Appl. Phys.* **1998**, 84, 848.
- [33] J. C. Scott, G. G. Malliaras, *Chem. Phys. Lett.* **1998**, 299, 115.
- [34] L. Bürgi, T. J. Richards, R. H. Friend, H. Sirringhaus, *J. Appl. Phys.* **2003**, 94, 6129.
- [35] B. H. Hamadani, D. Natelson, *J. Appl. Phys.* **2005**, 97, 064 508.
- [36] V. Ramamurthy, K. Venkatesan, *Chem. Rev.* **1987**, 87, 433.